New trends in spectroscopy of solid nitrogen

(Topical Review)

E. Savchenko[1], I. Khyzhniy[1], and V. Bondybey[2]

[1]*B. Verkin Institute for Low Temperature Physics and Engineering of the National Academy of Sciences of Ukraine,*
47 Nauki Ave., Kharkiv 61103, Ukraine

[2]*Lehrstuhl für Physikalische Chemie TUM, Garching b. München 85747, Germany*
E-mail: elena.savchenko@gmail.com

This topical review presents new trends in emission spectroscopy of solid nitrogen. Developed approach to study of charged centers and their role in radiation-induced phenomena as well as relaxation processes is discussed. The emission spectroscopy elaborated incorporates correlated in real time detection of several relaxation emission — optical photons, electrons and emission of particles. Key details of this approach applied in research of pre-irradiated by electron beam solid nitrogen and nitrogen–helium nanoclusters grown by a gas jet condensation technique are given. New methods — nonstationary luminescence and nonstationary desorption, designed to study ion-electron recombination reactions — are briefly presented. The selected recent results obtained employing this approach and emission spectroscopy techniques to study the charge related phenomena in condensed nitrogen are summarized. Main attention is given to detection of polyatomic ionic centers containing four and three nitrogen atoms: N_4^+, N_3^+, N_3^-. Their part played in radiation-induced phenomena and relaxation processes, in particular desorption, is discussed.

Keywords: solid nitrogen, nitrogen anions and cations, recombination reactions, neutralization, tetranitrogen, desorption.

Contents

1. Introduction

Nitrogen solids gained general recognition as classical model molecular crystals and their properties were reviewed in [1,2]. The keen interest in the research of electronic structure, stability of nitrogen polyatomic species and ways of their formation is related to the problem of polynitrogen compounds considered as environment-friendly high energy-density materials HEDM [3–5]. In this context it is noteworthy to mention a cycle of studies performed with such an exotic HEDM as grown from discharge nitrogen-containing nanoclusters immersed in superfluid He, e.g. [6–12]. High local concentration of stabilized nitrogen atoms (up to $2 \cdot 10^{21}$ cm^{-3}) has been obtained in porous nitrogen nanoclusters in superfluid helium [7,11]. Nitrogen and nitrogen-rich, so-called ices present in large abundance in outer space [13], where they are exposed to solar wind and galactic cosmic rays, have become objects of

laboratory simulation of astrophysical processes [14–20]. Solid nitrogen itself is rich in applications: it is used as matrix in radiation chemistry [21], as moderator [22] and source of nitrogen plasma [23]. Understanding the processes underlying desorption from solid nitrogen, is essential for ensuring the safe functioning of high-energy charged particle accelerators incorporating elements operating at liquid-helium temperature [24]. Thin films of residual gases (mostly nitrogen), condensed on cryogenic surfaces, are subjected to intense ionizing radiation, and radiation-induced desorption can greatly affect the operating conditions. There were a number of studies on radiation induced desorption [25–32] but only recently spectral methods have been successfully applied [33–35]. In all mentioned fields of science and applications radiation effects, energy transformation, storage, and its release are the focus of studies and among the methods used spectroscopy is one of the most effective.

Optical spectroscopy of solid nitrogen has a long story. Molecular electronic states of solid nitrogen and exciton-phonon interaction have been the objective of much research [36–43]. Numerous studies have focused on radiation effects — dissociation of N_2 molecule and synthesis of polynitrogen species. The formation of N radicals in solid nitrogen grown from discharge and irradiated with an electron beam was detected in the first studies related to clearing up emitters of Polar Aurora [44,45]. Later studies, e.g. [46–48], revealed an interaction of N radicals with the surrounding molecules in the lattice and formation of a weakly bound triatomic molecule, N_2–N. The laboratory studies of radiation-induced processes in astrophysical ices detected the azide radical N_3 in solid nitrogen exposed to energetic particles, e.g., protons [14], electrons [15] and VUV photons [16]. In most of studies radiation effects in solid N_2 were explored and considered in terms of neutral electronic excitations and their interactions. In spite of the fact that ionic compounds such as N_3^+ and N_4^+ were detected in pure solid nitrogen [49] and N_4^+ in the nitrogen-doped neon matrix [50,51] almost 30 years ago, the fascinating problem of charged (ionic) species dynamics and their role in a variety of radiation-induced phenomena remained poorly investigated. Active research in this direction has been undertaken in recent years [33–35,52–62]. First manifestation of charged centers accumulation and induced by their recombination features in luminescence spectra of nitrogen-doped rare gas solids were published in [63,64]. Direct detection of electron accumulation in solid nitrogen under irradiation was accomplished using activation spectroscopy current method — thermally stimulated exoelectron emission (TSEE) [65].

In this review we present new trends in spectroscopy of solid nitrogen. Much progress towards an understanding of the role of charged centers in radiation-induced phenomena and relaxation processes has been achived due to introduction of a new approach and new methods. Most of earlier

studies used an absorption spectroscopy in the infrared range — Fourier-transform infrared (FTIR) spectroscopy and mass spectroscopy. The method of activation spectroscopy — thermally stimulated luminescence (TSL) — was first applied to solid nitrogen by Brocklehurst and Pimentel [66]. The total yield of TSL from solid nitrogen preliminary exposed to an electron beam was detected and interpreted as a recombination of neutral N atoms followed by excited molecule formation (presumably in $A^3\Sigma_u^+$ state), in other words, as chemiluminescence. The TSL of solid nitrogen grown from discharge was registered in the range of atomic transition $^2D \rightarrow ^4S$ [67]. We have already referred to numerous studies, e.g. [6–12], of nitrogen enriched impurity-helium condensates (IHCs) grown by a gas jet condensation technique suggested by Gordon and coworkers [6] and developed in a new field of activity focused on N radicals. It should be emphasized that TSL could come not only from recombination of neutral atoms but also from the recombination of charged centers — the process well-known in a variety of materials [68]. However, this mechanism of TSL production via neutralization reactions has not been considered for a long time when discussing the results of studying relaxation processes in solid nitrogen.

In order to distinguish between recombination of neutral and charged particles, it is necessary to involve current methods, such as TSEE or measurements of thermally stimulated currents TSC along with optical methods of activation spectroscopy. A new approach involving the use of current spectroscopy techniques has been developed and implemented in the research of radiation effects in solid nitrogen exposed to an electron beam [33–35,53,55,56,58–60] and in the studies of IHCs [54,57,62,69]. New methods of nonstationary spectroscopy to probe charged species in irradiated solid nitrogen were implemented in [34,53,55,59]. The developed techniques and the results obtained will be discussed in the next sections. Main attention is given to detection of polyatomic ionic species containing four and three nitrogen atoms: N_4^+, N_3^+, N_3^-. Their part played in radiation-induced phenomena and relaxation processes, in particular desorption, is also discussed.

2. New experimental approach and techniques

2.1. Detection of relaxation emissions: photons, electrons, particles

Charge carriers generated in dielectric media by ionizing radiation could survive being trapped or self-trapped. Electrons in low-temperature α-phase of solid nitrogen are highly mobile [70]. The most probable structure trapping sites of electrons are thought to be vacancies or vacancy clusters in view of the negative electron affinity $E_e = -0.8$ eV [71] of solid nitrogen. Species with positive electron affinity (like radiation induced nitrogen species, e.g. the azide radical N_3, as well as impurity O atoms and O_2 molecules) form deep traps. The electrons may be promoted from

shallow and deep traps into the conduction band at heating or irradiation by photons of appropriate energy. Then they can either neutralize positively charged ions yielding TSL/PSL, or be registered with an electrode kept at a positive potential, as TSEE/PSEE or TSC/PSC. Third relaxation emission — emission of particles from the surface of pre-irradiated with an electron beam solid nitrogen, so-called "post-desorption", was first detected in [72]. Its key feature was nonmonotonous behavior of particle yield upon warm up of the sample — an intense peak of post-desorption was detected at temperatures much lower than the characteristic temperature of solid nitrogen sublimation. A correlation between the particle and electron emissions clearly demonstrated a dominant role of charge recombination reactions in this phenomenon.

In view of the sensitive dependence of the TSEE/PSEE, TSL/PSL, post-desorption and other phenomena upon the sample structure, impurity concentration, and other variables, there is obvious need to perform time correlated measurements of all the thermally/optically stimulated emissions simultaneously, on the same sample to get reliable results and come to solid conclusions. Such an approach was implemented in the studies of relaxation dynamics and the role of charge carriers in films of solid nitrogen and IHCs.

2.2. Activation spectroscopy techniques applied to solid N_2

The experimental methods of optical and current activation spectroscopy of solidified gases have been described in detail in Sec. 7 of Ref. 73 along with the selected results of rare gas solids (RGS) studies performed using this approach. Here, we give a brief account of the procedures and new technique — nonstationary desorption (NsD) [34] in parallel with nonstationary luminescence (NsL) [74]. These techniques were designed to reveal charged species

contribution to desorption and luminescence. The experimental setup used for emission spectroscopy studies is shown in Fig. 1. The films of solid nitrogen are formed by deposition of pure gas onto a cold metal substrate mounted on a liquid He cryostat tank. Samples are irradiated with an electron beam of subthreshold energy to exclude the knock-on defect formation and sputtering. By varying electron energy and, therefore, changing the penetration depth it is possible to probe solid nitrogen films "layer-by-layer" what enables to discriminate surface and bulk emitting centers.

The required temperature measured with a Si sensor can be set using the heater. The preset heating rate of the sample is controlled by the program. The luminescence spectra are recorded simultaneously in VUV and visible range (from 50 nm up to 1100 nm) using two ports of the experimental chamber. Additional chamber port is used in experiments on photon-stimulated emissions — PSEE and PSL from pre-irradiated nitrogen films. The total yield of desorbing particles is monitored with an ionization detector (a Bayard–Alpert gauge) simultaneously with the yields of spectrally resolved TSL and TSEE.

2.3. Nonstationary desorption and luminescence techniques

The developed nonstationary desorption and luminescence techniques are aimed to reveal the role of charged species recombination, viz. neutralization reactions, in relaxation cascades and stimulation of electronically induced phenomena, specifically desorption from the surface of irradiated solids. At low temperatures when some part of electrons produced under irradiation appeared to be trapped in the lattice, the corresponding part of the positively charged ionic species, that managed to avoid fast recombination, remain stable. The main idea of these methods is to create conditions when localized charge car-
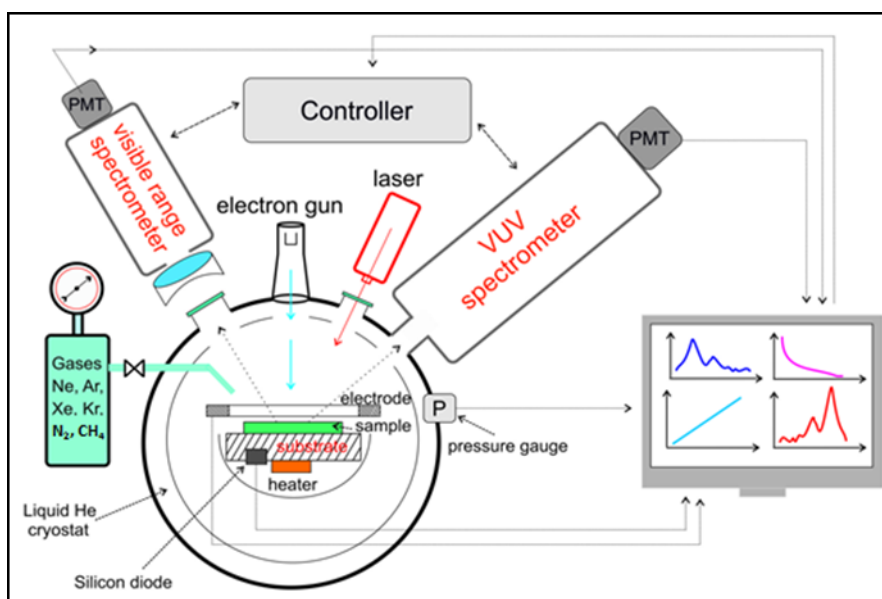

Fig. 1. (Color online) Scheme of the experimental setup for activation spectroscopy study of solid N_2.

riers of different signs come into play. For the purpose at the first stage the charged species of interest are generated with an electron beam of a high current density. In different experiments current densities from 1 mA/cm^2 up to 5 mA/cm^2 have been used. The irradiation was carried out until the corresponding emission was saturated. As a rule the temperature increase under beam did not exceed 0.4 K. At the second stage the ionic species generated were probed by NsD and NsL which were induced by a low-density electron beam under gradual heating. An intensity of probing electron beam was set by an order of magnitude lower to minimize the production of new ions. Electrons released from the progressively deeper traps, *in situ* "injected", recombine with positively charged species enhancing yields of particles and photons and thus contributing to the NsD and NsL. This contribution to the nonstationary emissions results in nonmonotonic temperature evolution of the particle and photon yields. The shape of these curves is determined by the energy levels of electron traps in the sample, from which the electrons are released upon heating. The controlled heating was performed at the same rate (of 6 K/min) at which the TSEE yield was measured to trace their correlation. The methods of NsL and NsD were employed to advantage in the experiments that found desorption of excited atoms and molecules. Relevant results will be discussed in the following sections.

3. Optical and current spectroscopy of nitrogen-containing nanoclusters

A gas jet condensation technique used to accumulate nitrogen nanoclusters in superfluid He was described in detail, e.g. in [6,75]. A gas mixture of N_2 (1%) and He or with the addition of any heavier inert gases (N_2/Ar/He, N_2/Xe/He) was transported by a gas handling system to the cryogenic part. Nitrogen atoms were produced by dissociation of N_2 molecules by using a high power radiofrequency (rf) discharge ($f \sim 40$ MHz, $P \sim 40$ W) applied to electrodes placed around the quartz capillary carrying the mixed gases. The resulting jet of helium gas with nitrogen particles emerging from the quartz capillary was directed onto the surface of superfluid ^{4}He contained in a glass beaker. The gas jet flux was about of $4 \cdot 10^{19}$ particles/s. Figure 2 presents the scheme of experimental setup for preparation and study of IHC according [57].

During the cooling of the gas jet, at first nitrogen nanoclusters are formed. When the temperature gets lower, He atoms are adsorbed on the surface of the nitrogen clusters. The temperature during sample preparation was kept about 1.5 K. As the jet penetrated the surface of the liquid He, a macroscopic snow-like objects consisting of nitrogen nanoclusters isolated by solid He shells were created. Warming the sample when removed from bulk liquid He initiates evaporation of helium layers, giving
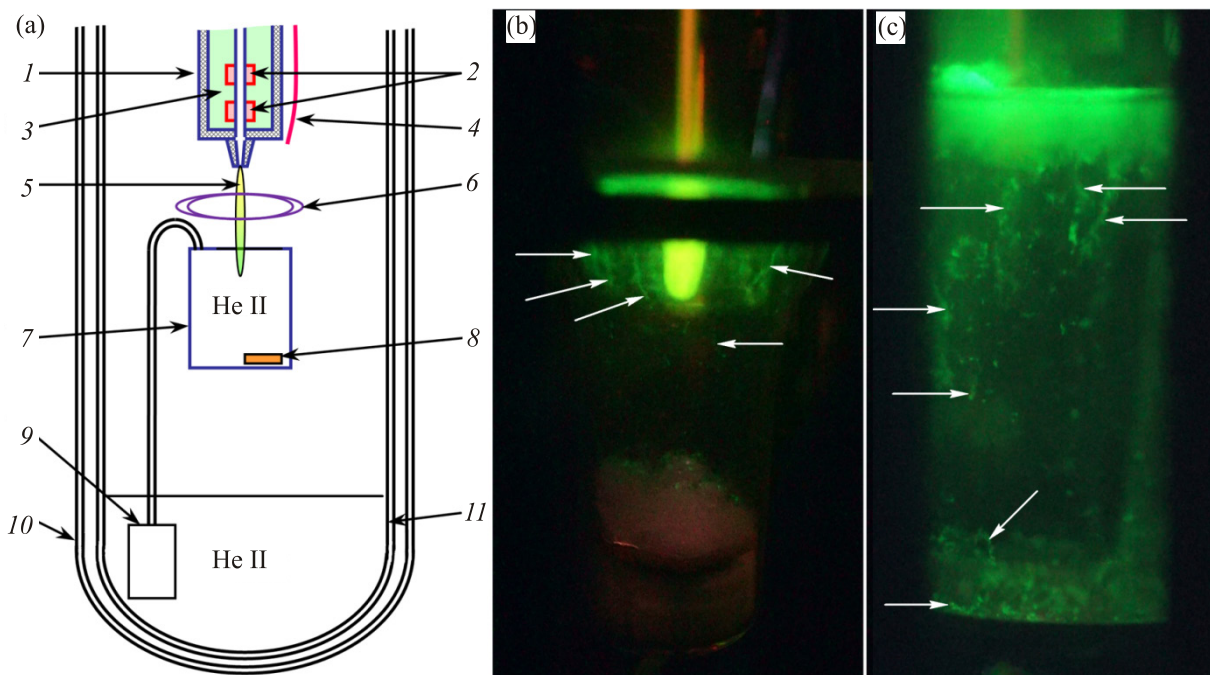

Fig. 2. (Color online) (a) Scheme of experimental setup for preparation and study of IHC samples: atom source (*1*); electrodes for rf discharge (*2*); liquid nitrogen (*3*); optical fiber (*4*); gas jet (*5*); ion collector (*6*); glass beaker filled with superfluid helium (*7*); thermometer (*8*); fountain pump (*9*); nitrogen glass dewar (*10*); helium glass dewar (*11*); (b) and (c) IHC sample preparation by condensation of the gas jet passed through an rf discharge (a gas mixture [N_2]/[He] = 1/100 and [N_2]/[Xe]/[He] = 1/1/400, correspondingly). White arrows point to filament-like structures [57].

rise to direct contact between neighboring cluster surfaces, accompanied by recombination of the reactive species. During the sample warm-up the TSL spectra were repeatedly detected. The glass dewars and beaker restricted the accessible spectral range from 325 to 1100 nm.

In the study [69] measurements of electrical currents accompanying heating and destruction of nitrogen–helium samples was first introduced. Currents were collected on an electrode held at the positive potential (+9 V). In this experiment the detecting electrode was placed at the bottom of a glass beaker filled with superfluid helium. A signal collected by the electrode was digitized with picoammeter (Keithley 6485). Measurements of current were performed in correlated fashion with a total yield of luminescence. Figure 3 shows the first results of current detection from IHC.

In further experiments [54] it was directly demonstrated that currents can be observed only from the IHCs prepared with an rf discharge. The authors found that the destruction of impurity–helium condensates induced by evaporation of liquid helium from the beaker is accompanied with pressure and luminescence peaks, and current pulses of positive and negative polarities. As an example, Fig. 4(a) shows the temporal dependences of the temperature, pressure, current, and integrated luminescence intensity during destruction of the sample prepared from a gas mixtures $[N_2]/[Xe]/[He] = 1/1/400$. Correlation of these peaks suggests that charged species of both signs are strongly involved in the relaxation dynamics.

The carriers of negative charge were supposed to be electrons, while the positively charged particles are most likely to be nitrogen cations, as suggested in [57]. Note, that N_3^+ and N_4^+ cations were detected in a rf glow discharge sustained in a N_2/He gas mixture [76]. Two mechanisms of nanocluster charging were proposed. The first one is trapping electrons and positive ions by nanoclusters growing in the cold jet passed through a radiofrequency discharge. The
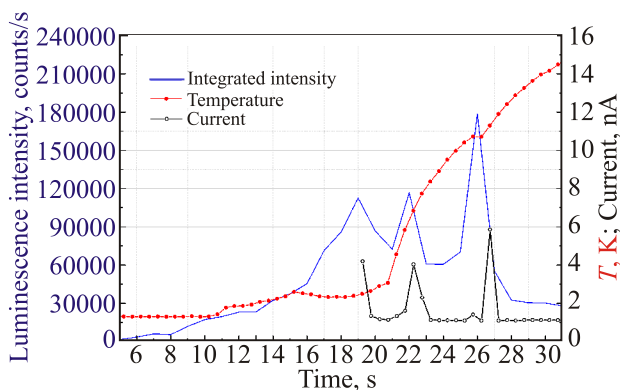

Fig. 4. (Color online) (a) The temporal dependences of the temperature (*1*), pressure (*2*), current (*3*), and integrated luminescence intensity (*4*) during destruction of sample prepared from a gas mixture $[N_2]/[Xe]/[He] = 1/1/400$ passed through an rf discharge zone. The orange vertical line shows the time when liquid helium had completely evaporated from the beaker. (b) Photo of the third flash (at $t = 323$ s) [54].

second mechanism, by the authors' opinion, consists in capture of electrons from the contacting surfaces by metastable $N_2(A^3\Sigma)$ molecule. Its interaction with surfaces followed by forming an intermediate shape resonance $N_2^-(^2\Pi_g)$ was considered for the case of dielectric in [77]. This mechanism results in electrostatic charging the IHC fragments and provides a charge separation of nanoclusters.

Recently the same group of authors elaborated impedance spectroscopy technique in addition to optical and current spectroscopy for studying processes during destruction of impurity–helium condensates [62]. A planar capacitive sensor had been chosen to measure an impedance of IHC samples. Fringing electric field sensor was adopted to the beaker cross-section. A sinusoidal signal source of the amplitude 5 V was used. The sample impedance was measured every 0.4 s at fixed frequency (equal 2.7 or 3 kHz). As the authors note, the efficient penetration length of the sensor is relatively small (0.55 mm by estimation) that is the main drawback of such a construction of fringing electric field sensors. However it was quite sensitive to detect charged species within the efficient volume of the sensor (0.14 cm^3).

As an illustration, Fig. 5 shows the temporal dependences of the temperature, luminescence intensity, resistance and capacity, corresponding to real and imaginary parts of impedance, during a destruction of sample prepared from $[N_2]/[Xe]/[He] = 1/1/400$ gas mixture. Note, that measurements of the temperature, current and impedance during rf discharge were not possible because of strong electric field interference but combination of these techniques appeared to be quite effective to study destruction of IHC samples. Detection of current pulses as well as

Fig. 3. (Color online) The time dependence of the current (black line with hollow circles), the integrated luminescence intensity (blue line), and the temperature (red line with solid circles) detected during warm-up and destruction of a nitrogen–helium sample [69].
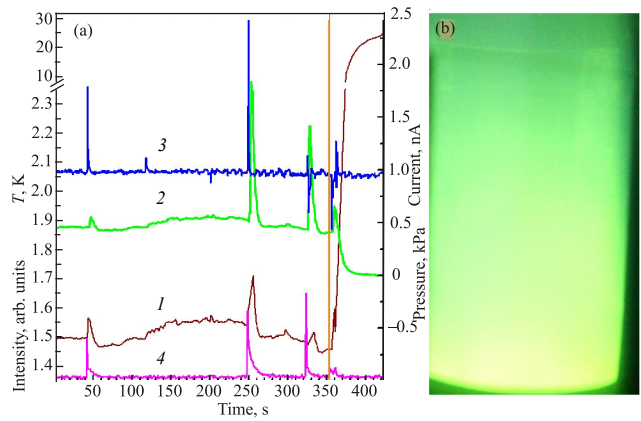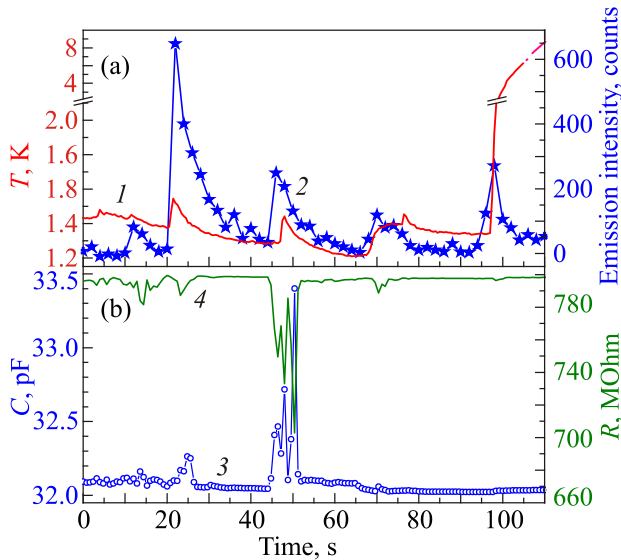
Fig. 5. (Color online) Destruction of sample prepared from $[N_2]/[Xe]/[He] = 1/1/400$ gas mixture: temporal dependences of the temperature (*1*) and luminescence intensity (*2*) (a); temporal dependences of the capacity (*3*) and resistance (*4*) (b) [62].

sharp decreases of a real part of the impedance provided clear evidence of charged fragments formation in the IHCs.

4. Experimental detection of polynitrogen ions and stimulated processes

4.1. N_4^+: *fingerprints in the emission spectra*

In this section we will focus on experimental findings indicating the formation of the N_4^+ cation in solid N_2, its stability and part in relaxation dynamics. The information about species formed during exposure to an electron beam and the relaxation cascades was obtained from cathodoluminescence (CL) spectra, their evolution under irradiation and behavior of time-correlated relaxation emissions. Figure 6 illustrates the typical CL spectrum of solid nitrogen in the VUV range. The most intense bands are the singlet molecular progression $a'^1\Sigma_u^- \to X^1\Sigma_g^+$ and intercombination transition $A^3\Sigma_u^+ \to X^1\Sigma_g^+$. The positions of the vibrational bands of both progressions are in good agreement with those observed in the early studies of VUV luminescence of solid N_2 [36,37,41–43].

All the vibrational bands of both progressions show a matrix shift towards lower energy in comparison with the gas phase spectra indicating the bulk origin of the emitting species. An emission from the $a'^1\Sigma_u^-$ state was identified in earlier studies as emission related to excitons [36,37,41–43]. However monitoring of the CL spectra temporal evolution has revealed an increase in the luminescence intensity with an exposure time (shown in Fig. 7) pointing to accumulation of radiation-induced centers responsible for this molecular emission [53].
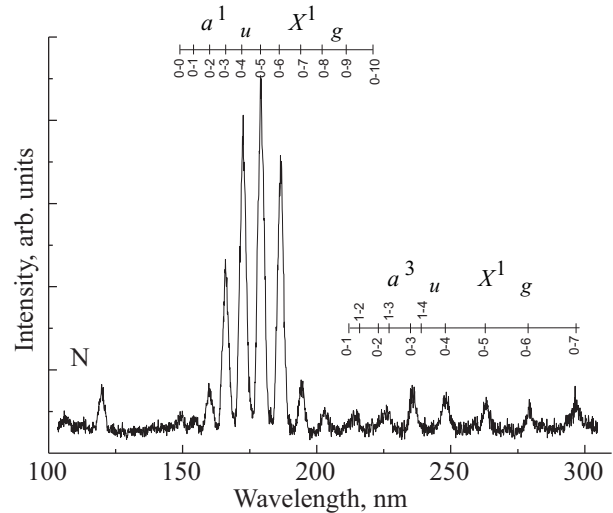

Fig. 6. Cathodoluminescence of solid nitrogen in the VUV range.

At the beginning slow rise of the recombination emission intensity was observed followed by faster increase and then saturation. The first phase of dose dependence (slow rise) corresponds mainly to filling of electron traps. The following phase (faster rise with saturation) can be described by the simple expression:

$$I(t) = I_{sat}\left[1 - \exp\left(-t/\tau\right)\right] \tag{1}$$

with the characteristic $\tau \approx 250$ s. I_{sat} corresponds to the intensity value upon reaching saturation. Such a behavior indicates an accumulation of radiation-induced centers which were supposed to be N_4^+ cations [53].

Effective test of charged centers is activation spectroscopy based on escaping of trapped electrons stimulated by heating or by photons. During irradiation the electron beam energy is absorbed by the sample and after switching off the excitation certain part of it remains stored in the solid. The energy storing centers could be trapped or self-trapped holes, trapped electrons, radicals, dopant ionic species and
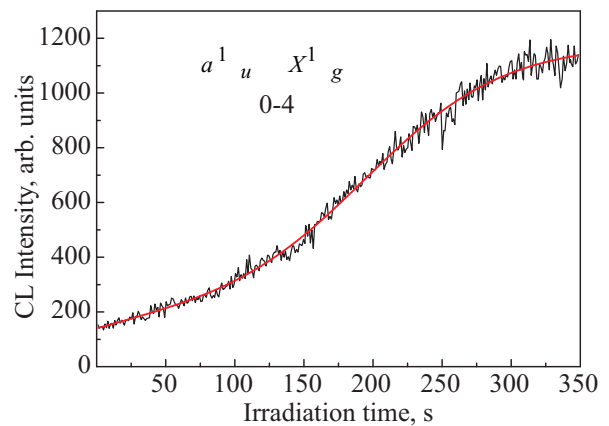

Fig. 7. Dose dependence of the $a'^1\Sigma_u^- \to X^1\Sigma_g^+$ progression intensity shown in the example of the 0-4 band. Red line — fit.

their fragments. As long as the temperature is maintained low the charged centers are separated in the sample and energy relaxation processes cannot start. Heating or irradiation with photons activates relaxation cascades and releases some part of the stored energy. The electrons promoted to the conduction band from some traps are highly mobile in the α-phase of solid nitrogen [70]. Some of them can escape from the surface and be detected as thermally stimulated exoelectron emission TSEE. A competing relaxation channel is recombination of the released electrons with positively charged ionic species: self-trapped/trapped holes and other cations. Neutralization reactions of charge centers result in thermally stimulated emission of photons — thermally stimulated luminescence (TSL). The information about the ionic species survived in the preliminary irradiated solid and about relaxation processes has been obtained from the measurements of spectrally resolved TSL [53,55].

Comparison of the TSEE yield measured simultaneously with TSL detected at wavelengths of the $a'^1\Sigma_u^- \to X^1\Sigma_g^+$ progression is shown in Fig. 8 on the example of a 0-4 molecular band. There is a pronounced TSEE peak at about 16 K with a weak shoulder near 13 K yield. The spectrally resolved TSL yield exhibits a wide feature in the same temperature range (12−18 K). Correlation of the molecular band with TSEE yield at low temperatures suggests that primary ionic centers responsible for the $a'^1\Sigma_u^- \to X^1\Sigma_g^+$ molecular emission are neutralized by the released electrons. In view of localized character of positive charge carriers in solid nitrogen [78], it was suggested that holes are self-trapped due to interaction with phonons [53] and N_4^+ cation is formed in course of the dimerization reaction:

$$N_2^+ + N_2 \to N_4^+. \tag{2}$$

The dimerization reaction with N_4^+ formation was also observed in supersonic nitrogen jet below 20 K [79].

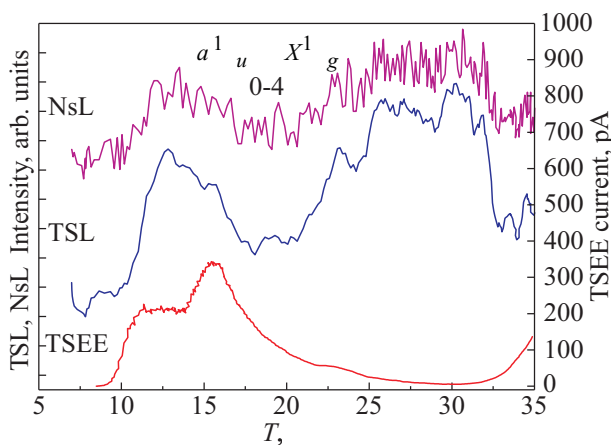The second TSL peak at 28 K has no corresponding feature in the TSEE yield. However, formation of the $a'^1\Sigma_u^-$ state via atom-atom recombination in a pre-irradiated sample is unlikely taking into account that its dissociation limit is formed by two nitrogen atoms in excited states: $N(^2D) + N(^2D)$ [80] and the 28 K TSL peak cannot be explained by the recombination of nitrogen atoms. It was suggested that this peak is caused by neutralization of close ion-electron pairs $N_4^+ + e^-$. This process does not contribute to TSEE yield because of much higher probability for released electrons to recombine with neighboring N_4^+ cation than to reach the sample surface. The NsL method was implemented to test the hypothesis [53]. For ionic species generation a solid nitrogen film was first irradiated with a 1 keV electron beam (6 mA/cm^2) and then the sample was probed with a 1 keV beam of 1 mA/cm^2 upon gradual heating. The NsL yield measured at a wavelength of 0-4 molecular transition of the $a'^1\Sigma_u^- \to X^1\Sigma_g^+$ progression is shown in Fig. 8. The observed correlation of NsL and TSL in the entire temperature range supports the idea that the $a'^1\Sigma_u^- \to X^1\Sigma_g^+$ radiative transition is induced by neutralization reaction.

The neutralization of N_4^+ results in the population of excited molecular states. Relaxation can occur via transition structures for fragmentation [3]. The barrier height for fragmentation depends on the electronic states of N_2^* involved. A theoretical study undertaken in [81] for the $N_4(D_{2h})$ configuration predicted no barrier for the state with the dissociation limit: $N_2(a'^1\Sigma_u^-) + N_2(a'^1\Sigma_u^-)$ as shown in Fig. 9.

Therefore it can be expected that the neutralization of the self-trapped holes results in the emergence of molecules in the lowest excited singlet states, followed by their radiative decay by the reaction

$$N_4^+ + e^- \to N_4^* \to N_2^*(a'^1\Sigma_u^-) + N_2^*(a'^1\Sigma_u^-) +$$

$$+ \Delta E_1 \to N_2 + N_2 + 2h\nu_1 + \Delta E_2. \tag{3}$$
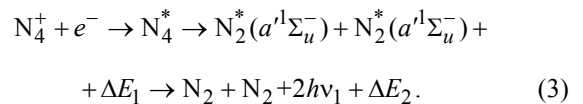
Additional evidence of effective N_4^+ formation and accumulation in solid nitrogen under electron beam was demonstrated in [55] by means of activation spectroscopy

Fig. 8. TSL detected at a wavelength of the 0-4 vibrational molecular band of the $a'^1\Sigma_u^- \to X^1\Sigma_g^+$ series, the TSEE yield and spectrally resolved NsL of solid nitrogen.
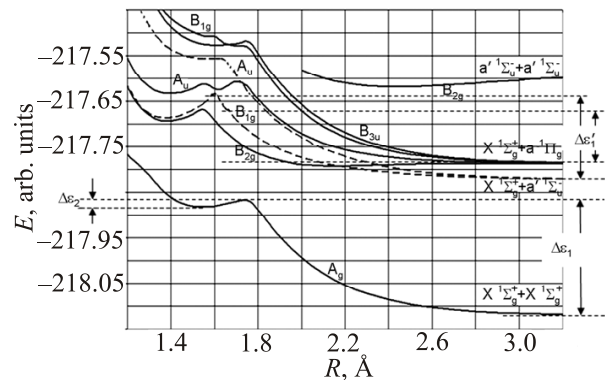

Fig. 9. Dependence of the $N_4(D_{2h})$ system energy on the coordinate R [81].

methods based on photon-stimulated release of electrons (PSEE and PSL). Relevant results will be given in the next section.

Reaction of dissociative recombination (2) represents the so-called "cage exit" [82] scenario when the excited N_2^* molecule exits the parent lattice "cage" where cation N_4^+ has recombined with an electron. However, there could be another relaxation scenario after dissociation. The excited N_2^* molecule could relax with a ground state N_2 molecule from the surroundings to form N_4^* and then N_4:

$$N_4^+ + e^- \rightarrow N_4^{**} \rightarrow N_2^* + N_2 + \Delta E_3 \rightarrow N_4^* \rightarrow N_4 + h\nu_2 + \Delta E_4.$$
(4)
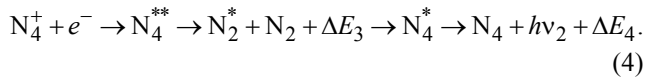
This scenario can be referred to as "cage effect" which confines the reaction products in the parent lattice "cage". Coexistence of scenarios (3) and (4) of N_4^+ neutralization has been proposed in [59]. Relaxation paths after neutralization and their branching are defined by potential curves of N_4 cluster and barriers for dissociation. It was shown theoretically [81] that for an N_4 cluster of D_{2h} symmetry the population of $^1B_{2u}$ state formed from $N_2(^3\Sigma_u^+)$ and $N_2(^3\Delta_u)$ states may result in a radiative transition into the ground state ^1A_g at ≈ 3 eV. In this spectral region, the luminescence band was recorded at 360 nm even in the early work of [83]. It was clear that this band belongs to nitrogen species however, its identification remained a long-standing problem. Moreover this band overlaps with the peaks of the second positive system, which belong to the emission of nitrogen molecules desorbing in the excited state, as shown in [34]. To "isolate" this band, the CL spectrum in this range was detected at the conditions when the desorption was suppressed — at excitation of thick films with higher-energy electrons when bulk features dominate the spectrum. The behavior of the band in question was investigated by emission spectroscopy methods. It has been shown that this band is characterized by strong dose dependence as illustrated by Fig. 10.

Enhancement of this band with exposure time reveals its radiation nature and points to accumulation of radiation-induced centers responsible for the emission observed. An additional test showed that the shape of the CL band is similar to the shape of the TSL band as seen in Fig. 11.

Time-correlated measurements of spectrally-resolved TSL yield and yield of TSEE were performed and compared to the spectrally resolved NsL yield. Correlation of all these relaxation emissions directly proves that the 360 nm band appears as a result of neutralization reaction.

An important point is the absence of the 360 nm band in the TSL of matrix-isolated N_2 molecules indicating its connection to a complex nitrogen center including more than two atoms. Taking into account the experimental findings and theoretical prediction [81] it has been suggested
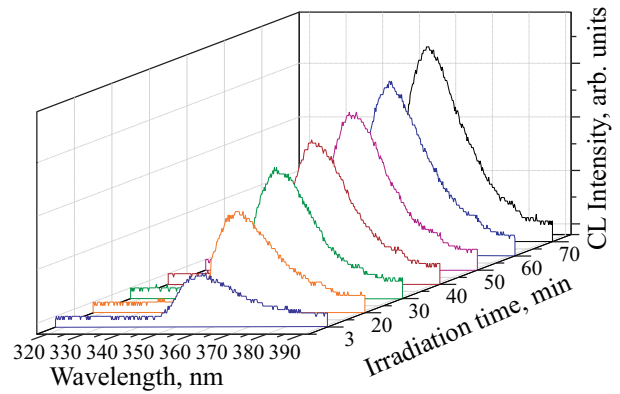

Fig. 10. Evolution of the 360 nm luminescence band with exposure time.

that the recombination of N_4^+ centers with electrons followed by excited N_4^* cluster formation is responsible for the detected 360 nm emission [59].

A broad band about $\lambda \approx 360$ nm was also detected in the luminescence of molecular nitrogen nanoclusters [84]. Optical spectra were observed during the destruction of nanoclusters accompanied by a rapid release of chemical energy stored in the samples. This emission was identified as corresponding to $^2A_g \rightarrow {}^1A_g$ transition of $N_4(D_{2h})$ polynitrogen center formed in IHC during the process of sample destruction accompanied by fast chemical reactions of nitrogen atoms and molecules. The authors assumed that the N_4 polynitrogen molecules are the product of the neutralization reaction of N_4^+ ions with electrons in N_2 nanoclusters [61]. It should be pointed out that N_4 neutral was detected by the neutralization-reionization mass-spectrometry [85–87]. The authors of [87] who performed both experiment and *ab initio* calculations concluded that the observed neutral cannot be the weakly bound van der Waals cluster $(N_2)_2$.

It is worth of note that, until now, there are no reliable experimental data on the N_4 and N_4^+ structure in solid
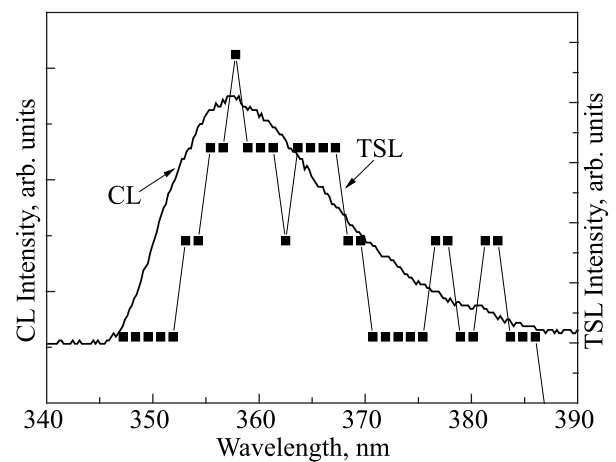

Fig. 11. Bands of spontaneous luminescence CL and stimulated luminescence TSL.
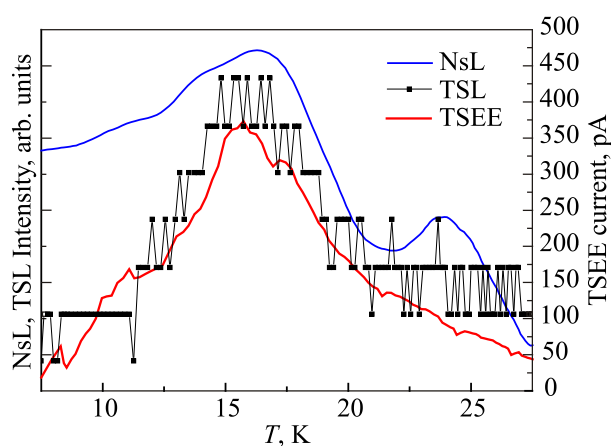
Fig. 12. TSL detected at 360 nm band maximum (middle curve), the TSEE yield (low curve) and the NsL yield measured at 360 nm.

nitrogen. So considering that, the need for further experimental and theoretical studies of the N_4 cluster formation is clear.

4.2. N_3^- and N_3^+: *their manifestation by emission spectroscopy*

The use of PSEE technique allowed finding "Fingerprints" of the anion N_3^- centers formation in pre-irradiated solid nitrogen. The sample preliminary irradiated with electrons was then subjected to continuous illumination. The energy of stimulating photons was selected in accordance with the electron affinity of N_3^- ($\chi = 2.76$ eV). Detection of the PSEE signal (Fig. 13) proves that deep electron traps were N_3^- anion centers efficiently formed in solid nitrogen pre-irradiated with an electron beam. A test of the TSEE yield after irradiation with photons confirms that 2.76 eV photons released electrons from deep traps, specifically from N_3^-.

Contribution of the N_3^- in electrostatic charging of pre-irradiated with electrons solid nitrogen was demonstrated [56]. In this study significant accumulation of negative charge with an accumulation of trapped electrons (no less
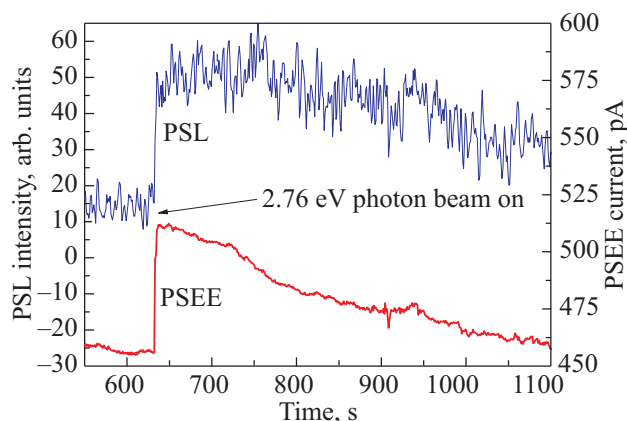

Fig. 13. Correlation of PSEE and PSL detected in (0-4) band of the $a'^1\Sigma_u^- \to X^1\Sigma_g^+$ transition.

than 10^{16} cm^{-3}) was revealed. Note that negatively charged species N_3^- have been also produced in N_2-dominated ices under proton bombardment and detected by IR spectroscopy in ices warmed to 35 K [88]. Stable N_3^- anions were detected in small nitrogen clusters embedded in helium droplets [89] using time-of-flight mass-spectroscopy.

In experiments [55], simultaneously with PSEE, stimulated by photons with an energy of 2.76 eV, the PSL yield was measured at wavelengths of the $a'^1\Sigma_u^- \to X^1\Sigma_g^+$ transition, as shown in Fig. 13 on the example of the vibrational band (0-4). In contrast to the discussed above experiments on thermal stimulation [53] the measurements of PSEE and PSL were performed at low temperature (5 K), when all processes of atom diffusion were frozen to exclude the population of the $a'^1\Sigma_u^-$ state via the recombination of two excited N* atoms in ^2D states. The observed clear correlation of PSL and PSEE proves the hole self-trapping with tetranitrogen cation N_4^+ formation, which is followed by the photon-stimulated dissociative recombination reaction of N_4^+ cations with electrons as described in previous section. The entire set of data [55] made it apparent that charges of both signs (N_3^- anions, N_4^+ cations and electrons) can be stored at low temperatures.

Along with N_4^+ one of the main products of nitrogen radiolysis is N_3^+ cation [3,4]. N_3^+ is a relatively stable molecular ion ($D_0 = 3.4$ eV) compared to N_4^+ ($D_0 = 1$ eV) [3]. Photoabsorptions by $N_3^+ - (N_2)_n$ complexes have been observed in clusters [90]. It was shown that the larger complexes essentially consist of an N_3^+ core surrounded by electrostatically bound N_2 ligands. Experiments on fast ion collision with icy surface of nitrogen revealed two series of positive ions: $(N_2)_n N_2^+$ and $(N_2)_n N^+$ with a predominance of small clusters [91]. The IR absorption measurements of the electron-bombarded pure solid N_2 [52] found the formation of N_3^+ cation, which was confirmed by the observed in VUV range electronic transitions $A^3\Pi_u \leftarrow X^3\Sigma_g^-$ of N_3^+ [52]. Formation of N_3^+ cations was also detected in CL spectrum of solid nitrogen shown in Fig. 14 [58]. The band $A^3\Pi_u(000) \to X^3\Sigma_g^-$ (000) at 281 nm has been registered against 0-6 band of the $A^3\Sigma_u^+ \to X^1\Sigma_g^+$ transition. A weak band at 273 nm in the CL spectrum was assigned to the $A^2\Sigma_u^+(000) \to X^2\Pi_g$ (000) transition of N_3 radical. Low intensity of this band in experiments [58] is likely due to efficient formation of N_3^- anions detected with PSEE technique as described above.

Experimental and theoretical data on formation of trinitrogen system were reviewed in [3,4]. The relative energies of the trinitrogen system in different states are schematically presented in Fig. 15.

It is worthy of note that the N(^4S) atom should first be excited into its ^2D state to be able to form a new chemical bond with N_2 and create N_3 neutral [3,4].

In view of essential role of electrons in relaxation processes information on neutralization reaction of N_3^+ is of vital importance. The study of this reaction performed at
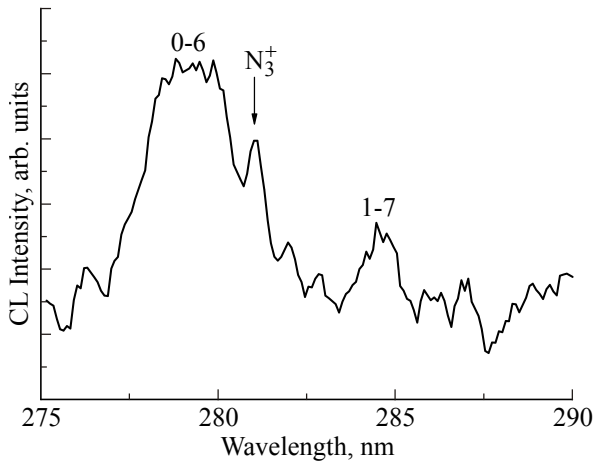
Fig. 14. Feature related to N_3^+ in the CL spectrum of solid nitrogen.

the heavy-ion storage ring CRYRING [92] revealed two exothermic channels — two-body and three-body:

$$N_3^+ + e^- \rightarrow N_2 + N + \Delta E_5, \qquad (5)$$

$$N_3^+ + e^- \rightarrow N + N + N + \Delta E_6. \qquad (6)$$

Both channels represent dissociative recombination reactions. In the case when the reactions (5) and (6) products are formed in the ground state, the energy release in the reaction (5) comprises $\Delta E_5 \sim 10.5$ eV and $\Delta E_6 \sim 0.7$ eV in the reaction (6). In view of that a strong propensity to dissociate via the $N_2 + N$ channel has been found [92]. A large amount of energy released in two-body channel (5) provides a basis for electronically stimulated processes — defect formation and desorption.
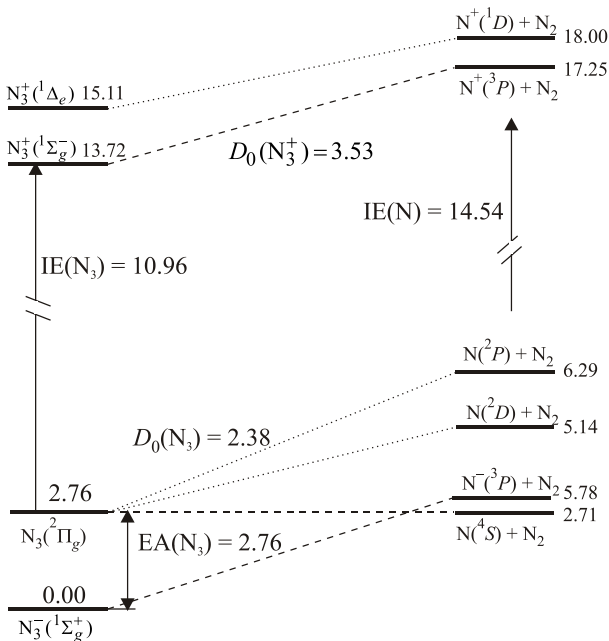

Fig. 15. Schematic representation of relative energies of the trinitrogen system by [3].

4.3. Charged species in electronically stimulated processes

Interesting feature of the α-group emission (N(^2D–^4S) transition) is its dose dependence observed in [35]. At the beginning, a slow rise of the recombination emission intensity was observed followed by a faster increase and then saturation. The excited N(^2D) atom may appear as a result of direct excitation of N(^4S) — product of N_2 molecule dissociation, under electron beam. Another possibility is the recombination of ground state nitrogen atoms followed by formation of electronically excited molecules $N_2(A^3\Sigma_u^+)$ and $N_2(A^5\Sigma_g^+)$. Energy transfer from these molecules to N(^4S) atoms can also result in the production of electronically excited N(^2D) atoms [94]. However the dose dependences of the α-group emission and the $A^3\Sigma_u^+ \rightarrow X^1\Sigma_g^+$ progression appeared to be different. Moreover the TSL of solid nitrogen recorded at the wavelength of the $^2D \rightarrow {}^4S$ transition shows only one low-temperature peak at about 15 K, in contrast to the TSL of matrix-isolated N_2 centers, in which the second TSL peak is also observed at higher temperatures [63] where mass diffusion processes come into play. In solid nitrogen the observed TSL peak correlates with the TSEE yield pointing to a connection of the atomic center N(^2D) generation with a charge recombination reaction. Recombination of N_2^+ with an electron cannot be responsible for the TSL in α-band of pure nitrogen because of hole self-trapping/trapping, while in N_2-doped rare-gas matrices the dissociative recombination of N_2^+ may result in creation of defect center N(^2D) [64] by analogy with the well-known dissociative recombination in a low-density nitrogen gas [93]. Ionic center N_4^+ dissociates into molecules at neutralization. The trapped holes — N_3^+ centres discussed above, look like good candidates for the neutralization process by reaction (5). The energy released in the channel (5), exceeds 10 eV which creates preconditions for dissociation with the emergence of N(^2D) center. Then ^2D excitation decays radiatively leaving a point defect N(^4S) in the nitrogen lattice.

A huge energy release in reaction (5) can also produce N atoms in higher states. Thus, in [34], reaction (5) was proposed as one of the possible mechanisms of the excited N* atom desorption of atoms in the $3s$ $^4P_{5/2-1/2}$ state. In this study two atomic lines were found at 120 and 113.4 nm. The distinctive feature of these lines is their coincidence with the gas phase spectrum within the accuracy of the measurements in [34]. Spectral line at 120 nm belongs to the $3s$ $^4P_{5/2-1/2} \rightarrow 2p^3$ $^4S_{3/2}$ transitions. Weaker line at 113.4 nm stems from the transitions $2p^4$ $^4P_{1/2-5/2} \rightarrow 2p^3$ $^4S_{3/2}$ transitions. Experiments on samples of different thickness and probing them in depth by changing the electron beam energy confirmed the connection of these emissions with the surface. Direct connection of 120 and 113.4 nm lines with charge recombination reactions was evidenced using NsD and NsL methods [60]. The relevant result is shown in Fig. 16.
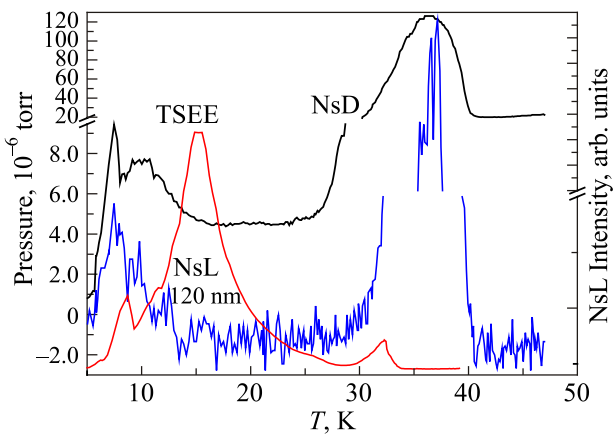
Fig. 16. NsL measured at 120 nm ($^4P \rightarrow {}^4S$ atomic transition) detected simultaneously with NsD (pressure curve) and TSEE yield.

The low-temperature peak near 8 K coincides with the position of the low-temperature peak of TSEE near 8 K indicating the connection of the 120 nm line with the neutralization process. As it was pointed $\Delta E_5 = 10.5$ eV can ensure the population of the $3s$ $^4P_{5/2-1/2}$ state with subsequent desorption of excited atoms. However ΔE_5 is insufficient for population of the $2p^4$ $^4P_{1/2-5/2}$ state that suggests another mechanism of highly excited atoms desorption. It was assumed [34,60] that creation of N^+ ions at the surface via core excitations followed by their neutralization may result in desorption of highly excited N^* atoms.

Similar approach was used in study of excited molecule desorption [34,35]. In the near UV range the emission of second positive system (2PS) was registered — the transitions between $C^3\Pi_u$ and $B^3\Pi_g$ excited molecular states (Fig. 17). The positions of the observed bands coincide with those detected in the gas phase nitrogen spectra. These bands were observed at 5 K in early study [83] and interpreted as stemming from freely rotated N_2^* molecules in solid nitrogen. But this assignment is in contradiction with the calculated height of barrier 35 K for rotation in the α-phase of solid N_2 where molecules are frozen [95].
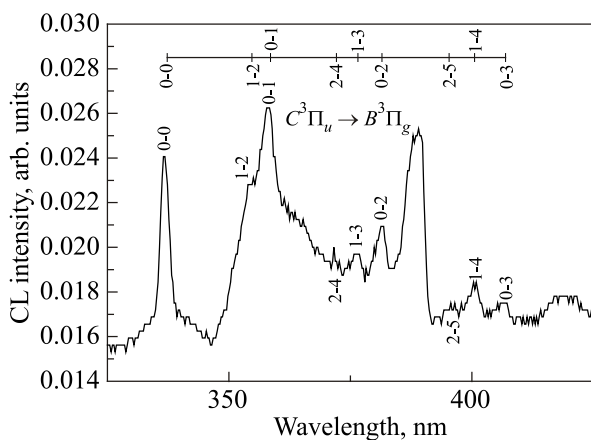

Fig. 17. The 2PS in luminescence of solid N_2 excited with 500 eV electron beam.

Measurements of the thickness dependence of the 2PS emission and probing with an electron beam established connection of these bands with the surface. It was concluded that the 2PS emission in solid nitrogen stems from N_2^* molecules desorbing in the excited $C^3\Pi_u$ state [34,35].

A blue matrix shift of the bands in Ne matrix in accordance with [96] supports the conclusion. Desorption of metastable nitrogen molecules stimulated by low-energy electrons was detected by time-of-flight technique in [29]. A study of dose-response behavior performed in [35] revealed the accumulation of centers responsible for the desorption of excited molecules and suggested the neutralization reaction of $(N_2)_2^+$ van der Waals dimer ions as the underlying process. Formation of $(N_2)_2^+$ ions under irradiation of a dense gas was investigated in a number of studies, e.g. [97–100]. First observation of photon emission due to electron-ion recombination of $(N_2)_2^+$ was reported in [101]. The neutralization of these ions by electrons resulted in the dissociative recombination reaction followed by an emission of the 2PS of N_2^* molecule: $C^3\Pi_u \rightarrow B^3\Pi_g$

$$N_4^+ + e^- \rightarrow N_2^*(C^3\Pi_u) + N_2 + h\nu. \qquad (7)$$
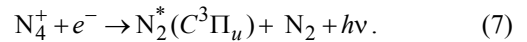
Contribution of charged centers in desorption of the excited nitrogen molecules was proved by measurements of the spectrally-resolved TSL on wavelengths of the 2PS. Simultaneously with the TSL the yields of TSEE and postdesorption (pressure curve) were measured.

Figure 18 presents all the time-correlated emissions. Photon yield – TSL, is shown on the example of 0-1 band of the $C^3\Pi_u \rightarrow B^3\Pi_g$ transition. Temperature behavior of the recombination luminescence strongly correlates with the TSEE current, indicating that the primary process, which underlies the desorption of excited nitrogen molecules, is the recombination of electron with positively charged ionic center $(N_2)_2^+$. The excited molecule at the surface experiences a repulsive interaction with neighbors because of negative electron affinity of solid nitrogen [71]
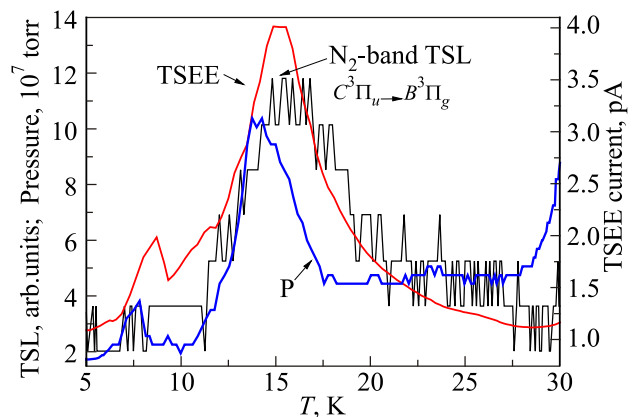

Fig. 18. Yields of the TSL measured in 0-1 band of the 2PS in comparison with concurrently detected TSEE yield and total yield of post-desorption.

that makes the so-called "cavity expulsion" mechanism efficient. It is interesting that neutral van der Waals clusters $(N_2)_2$ were also observed in dense gas [102] and in free icosahedral nitrogen clusters formed in supersonic jet [103].

Conclusions

In this topical review we have focused on the recent studies of charged centers generated in solid nitrogen and their role in radiation-induced phenomena. Numerous new methods employed to advantage of this reserch line are presented including current spectroscopy. The developed approach is based on time correlated emission spectroscopy with monitoring of optical photons, charge carriers and emission of particles. Recent findings in research of pre-irradiated by electron beam solid nitrogen and nitrogen-helium nanoclusters grown by a gas jet condensation technique are presented. Main attention is given to detection of polyatomic ionic centers containing four and three nitrogen atoms; N_4^+, N_3^+, N_3^-. Their photo- and thermostability were explored along with stimulated phenomena and relaxation processes. Examples of defect production and desorption induced by ion-electron reactions are discussed.

Acknowledgments

1. *Physics of Cryocrystals*, V.G. Manzhelii, Yu.A. Freiman, M.L. Klein, and A.A.Maradudin (eds.), AIP Pablisher, Woodbury, MA (1997).
2. T.A. Scott, *Phys. Rep. Phys. Lett. C* **27**, 89 (1976).
3. M.T. Nguyen, *Coord. Chem. Rev.* **244**, 93 (2003).
4. P.C. Samartzis and A.M. Wodtke, *Inter. Rev. Phys. Chem.* **25**, 527 (2006).
5. V.E. Zarko, *Combustion, Explos. Shock Waves* **46**, 121 (2010).
6. E.B. Gordon, L.P. Mezhov-Deglin, and O.F. Pugachev, *JETP Lett.* **19**, 63 (1974).
7. V. Kiryukhin, B. Keimer, R.E. Boltnev, V.V. Khmelenko, and E.B. Gordon, *Phys. Rev. Lett.* **79**, 1774 (1997).
8. R.E. Boltnev, I.N. Krushinskaya, A.A. Pelmenev, E.A. Popov, D.Yu. Stolyarov, and V.V. Khmelenko, *Fiz. Nizk. Temp.* **31**, 723 (2005) [*Low Temp. Phys.* **31**, 547 (2005)].
9. V. Kiryukhin, E.B. Bernard, V.V. Khmelenko, R.E. Boltnev, N.V. Krainyukova, and D.M. Lee, *Phys. Rev. Lett.* **98**, 195506 (2007).
10. N.V. Krainyukova, R.E. Boltnev, E.P. Bernard, V.V. Khmelenko, D.M. Lee, and V. Kiryukhin, *Phys. Rev. Lett.* **109**, 245505 (2012).
11. A. Meraki, P.T. McColgan, P.M. Rentzepis, R.Z. Li, D.M. Lee, and V.V. Khmelenko, *Phys. Rev. B* **95**, 1045026 (2017).
12. A. Meraki, P.M. McColgan, S. Sheludiakov, D.M. Lee, and V.V. Khmelenko, *Fiz. Nizk. Temp.* **45**, 862 (2019) [*Low Temp. Phys.* **45**, 737 (2019)].
13. R.N. Clark, R. Carlson, W. Grundy, and K. Noll, *Observed Ices in the Solar System*, in: *The Science of Solar System Ices*, M.S. Gudipati and J. Castillo-Rogez (eds.), Astrophysics and Space Science Library: Springer, New York (2012), vol. 356, p. 3.
14. R.L. Hudson and M.H. Moore, *Astrophys. J.* **568**, 1095 (2002).
15. C.S. Jamieson and R.I. Kaiser, *Chem. Phys. Lett.* **440**, 98 (2007).
16. Y.-J. Wu, C.Y.R. Wu, S.-L. Chou, M.-Y.Lin, H.-C. Lu, J.-I. Lo, and B.-M. Cheng, *Astrophys. J.* **746**, 175 (2012).
17. Ph. Boduch, A. Domaracka, D. Fulvio, T. Langlinay, X.Y. Lv, M.E. Palumbo, H. Rothard, and G. Strazzulla, *Astronomy & Astrophysics A* **544**, A30 (2012).
18. A.L.F. de Barros, E.F da Silveira, A. Bergantini, H. Rothard, and P. Boduch, *Astrophys. J.* **810**, 156 (2015).
19. C.K. Materese, D.P. Cruikshank, S.A. Sandford, H. Imanaka, and M. Nuevo, *Astrophys. J.* **812** 150 (2015).
20. M.E. Palumbo, G.A. Baratta, D. Fulvio, M. Garozzo, O. Gomis, G. Leto, F. Spinella, and G. Strazzulla, *J. Phys.: Conf. Ser.* **101**, 012002 (2008).
21. E.I. Grigoriev and L.I. Trakhtenberg, *Radiation-Chemical Processes in Solid Phase: Theory and Application*, CRC Press, Boca Raton, Florida (1996).
22. K. Ghandi and Y. Miyake, *Muon Interaction with Matter*, in: *Charge Particle and Photon Interaction with Matter: Recent Advances, Applications and Interfaces*, Y. Hatano, Y. Katsumura, and A. Mozumder (eds.), CRC Press, Boca Raton London, New York (2011), p. 169.
23. H. Niino, T. Sato, A. Narazaki, Y. Kawaguchi, and A. Yabe, *Appl. Surf. Sci.* **197−198**, 67 (2002).
24. H. Tratnik, N. Hilleret, and H Störl, *Vacuum* **81**, 731 (2007).
25. O. Ellegard, J. Schou, H. Sørensen, and P. Børgesen, *Surf. Sci.* **167**, 474 (1986).
26. R. Pedrys, D.J. Oostra, A. Haring, A.E. de Vries, and J. Schou, *Rad. Eff. Defects Solids* **109**, 239 (1989).
27. E. Hudel, E. Steinacker, and P. Feulner, *Surf. Sci.* **273**, 405 (1992).
28. O. Rakhovskaia, P. Wiethoff, and P. Feulner, *Nucl. Instrum. Methods Phys. Res. B* **101**, 169 (1995).
29. H. Shi, P. Cloutier, and L. Sanche, *Phys. Rev. B* **52**, 5385 (1995).
30. K.I. Öberg, E.F. van Dishoeck, and H. Linnartz, *Astronomy & Astrophysics* **496**, 281 (2009).
31. E.C. Fayolle, M. Bertin, C. Romanzin, H.A.M. Poderoso, L. Philippe, X. Michaut, P. Jeseck, H. Linnartz, K.I. Öberg, and J.-H. Fillion, *Astronomy & Astrophysics* **556**, A122 (2013).
32. E.M. Bringa and R.E. Johnson, *Ion Interactions with Solids: Astrophysical Applications*, in: *Solid State Astrochemistry*, V. Pirronello, J. Krelowski, and G. Manicò (eds.), Kluver Academic Publishers (2003), p. 357.
33. A.P. Barabashov, I.V. Khyzhniy, S.A. Uyutnov, M.A. Bludov, and E.V. Savchenko, *Fiz. Nizk. Temp.* **42**, 1512 (2016) [*Low Temp. Phys.* **42**, 1181 (2016)].
34. E.V. Savchenko, I.V. Khyzhniy, S.A. Uyutnov, M.A. Bludov, A.P. Barabashov, G.B. Gumenchuk, and V.E. Bondybey, *J. Luminescence* **191**, 73 (2017).

35. E. Savchenko, I. Khyzhniy, S. Uyutnov, A. Barabashov, G. Gumenchuk, A. Ponomaryov, and V. Bondybey, *Phys. Status Solidi C* **12**, 49 (2015).

36. I.Ya. Fugol', Yu.B. Poltoratskii, and E.V. Savchenko, *JETP Lett.* **24**, 3 (1976).

37. F. Coletti and A.M. Bonnot, *Chem. Phys. Lett.* **45**, 580 (1977).

38. E. Boursay and J.Y. Roncin, *Phys. Rev. Lett.* **26**, 308 (1971).

39. R. Haensel, E.E. Koch, N. Kosudi, U. Nielsen, and M. Skibowski, *Chem. Phys. Lett.* **9**, 548 (1971).

40. E. Boursay, V. Chandrasekharan, and P. Gürtler, *Phys. Rev. Lett.* **41**, 1516 (1978).

41. I.Ya. Fugol' and Yu.B. Poltoratskii, *Solid State Commun.* **30**, 497 (1979).

42. Yu.B. Poltoratskii, V.M. Stepanenko, and I.Ya. Fugol', *Fiz. Nizk. Temp.* **7**, 121 (1981) [*Sov. J. Low Temp. Phys.* **7**, 60 (1981)].

43. I.Ya. Fugol' and V.M. Stepanenko, *Solid State Communs.* **49**, 837 (1984).

44. L. Vegard, *Nature* **113**, 716 (1924).

45. J.C. McLennan and G.M. Shrum, *Proc. R. Soc. A* **106**, 138 (1924).

46. A.M. Bass and H.P. Broida, *Phys. Rev.* **101**, 1740 (1956).

47. M. Peyron, E.M. Hörl, H.W. Brown, and H.P. Broida, *J. Chem. Phys.* **30**, 1304 (1959).

48. O. Oehler, D.A. Smith, and K. Dressler, *J. Chem. Phys.* **66**, 2097 (1977).

49. R. Tian and J. Michl, *Faraday Discuss. Chem. Soc.* **86**, 113 (1988).

50. W.E. Thompson and M.E. Jacox, *J. Chem. Phys.* **93**, 3856 (1990).

51. L.B. Knight, Jr., K.D. Johannessen, D.C. Cobranchi, E.A. Earl, D. Feller, and E.R. Davidson, *J. Chem. Phys.* **87**, 885 (1987).

52. Y.-J. Wu, H.-F. Chen, S.-J. Chuang, and T.-P. Huang, *Astrophys. J.* **779**, 40 (2013).

53. E.V. Savchenko, I.V. Khyzhniy, S.A. Uyutnov, A.P. Barabashov, G.B. Gumenchuk, M.K. Beyer, A.N. Ponomaryov, and V.E. Bondybey, *J. Phys. Chem. A* **119**, 2475 (2015).

54. I.N. Krushinskaya, R.E. Boltnev, I.B. Bykhalo, A.A. Pelmenev, V.V. Khmelenko, and D.M. Lee, *Fiz. Nizk. Temp.* **41**, 541 (2015) [*Low Temp. Phys.* **41**, 419 (2015)].

55. E. Savchenko, I. Khyzhniy, S. Uyutnov, M. Bludov, G. Gumenchuk, and V. Bondybey, *Radiation Measurements* **90**, 1 (2016).

56. E. Savchenko, I. Khyzhniy, S. Uyutnov, M. Bludov, G. Gumenchuk, and V. Bondybey, *Phys. Status Solidi B* **253**, 2115 (2016).

57. A.A. Pelmenev, I.N. Krushinskaya, I.B. Bykhalo, and R.E. Boltnev, *Fiz. Nizk. Temp.* **42**, 289 (2016) [*Low Temp. Phys.* **42**, 224 (2016)].

58. E. Savchenko, I. Khyzhniy, S. Uyutnov, M. Bludov, A. Barabashov, G. Gumenchuk, and V. Bondybey, *IOP Conf. Ser: Materials Science and Engineering* **169**, 012007 (2017).

59. E. Savchenko, I. Khyzhniy, S. Uyutnov, M. Bludov, A. Barabashov, G. Gumenchuk and V. Bondybey, *J. Low Temp. Phys.* **187**, 62 (2017).

60. E. Savchenko, I. Khyzhniy, S. Uyutnov, M. Bludov, A. Barabashov, G. Gumenchuk, and V. Bondybey, *Nucl. Instr. Meth. B* **435**, 38 (2018).

61. P.T. McColgan, A. Meraki, R.E. Boltnev, S. Sheludiakov, D.M. Lee, and V.V. Khmelenko, *J. Phys.: Conf. Ser.* **969**, 012007 (2018).

62. A.A. Pelmenev, I.B. Bykhalo, I.N. Krushinskaya, and R.E. Boltnev, *Fiz. Nizk. Temp.* **45**, 318 (2019) [*Low Temp. Phys.* **45**, 276 (2019)].

63. A.N. Ponomaryov, E.V. Savchenko, G.B. Gumenchuk, I.V. Khizhniy, M. Frankowski, and V.E. Bondybey, *Fiz. Nizk. Temp.* **33**, 705 (2007) [*Low Temp. Phys.* **33**, 532 (2007)].

64. E.V. Savchenko, I.V. Khyzhniy, S.A. Uyutnov, G.B. Gumenchuk, and A.N. Ponomaryov, and V.E. Bondybey, *IOP Conf. Series: Materials Science and Engineering* **15**, 012082 (2010).

65. I. Khyzhniy, E. Savchenko, S. Uyutnov, G. Gumenchuk, A. Ponomaryov, and V. Bondybey, *Radiation Measurements* **45**, 353 (2010).

66. B. Brocklehurst and G. C. Pimentel, *J. Chem. Phys.* **36**, 2040 (1962).

67. E. Faure, B. Tribollet, F. Vincent, F. Valadier, and J. Janin, *Le J. de Phys. Lett.* **40**, L555 (1979).

68. D.R. Vij, in: *Luminescence of Solids: Thermoluminescence*, D.R. Vij (ed.), Plenum Press, New York (1998), p. 271.

69. R.E. Boltnev, I.B. Bykhalo, I.N. Krushinskaya, A.A. Pelmenev, V.V. Khmelenko, D.M. Lee, I.V. Khyzhniy, S.A. Uyutnov, E.V. Savchenko, A.N. Ponomaryov, G.B. Gumenchuk, and V.E. Bondybey, *Fiz. Nizk. Temp.* **39**, 580 (2013) [*Low Temp. Phys.* **39**, 451 (2013)].

70. V.G. Storchak, D.G. Eshchenko, J.H. Brewer, S.P. Cottrell, S.F.J. Cox, E. Karlsson, and R.W. Wappling, *J. Low Temp. Phys.* **122**, 527 (2001).

71. G. Bader, G. Perluzzo, L.G. Caron, and L. Sanche, *Phys. Rev. B* **30**, 78 (1984).

72. E.V. Savchenko, I.V. Khyzhniy, S.A. Uyutnov, A.N. Ponomaryov, G.B. Gumenchuk, and V.E. Bondybey, *Fiz. Nizk. Temp.* **39**, 574 (2013) [*Low Temp. Phys.* **39**, 446 (2013)].

73. M.A. Allodi, R.A. Baragiola, G.A. Baratta, M.A. Barucci, G.A. Blake, J.R. Brucato, C. Contreras, S.H. Cuylle, Ph. Boduch, D. Fulvio, M.S. Gudipati, S. Ioppolo, Z. Kaňuchová, A. Lignell, H. Linnartz, M.E. Palumbo, U. Raut, H. Rothard, F. Salama, E.V. Savchenko, E. Sciamma-O'Brien, G. Strazzulla, and G. Strazzulla, *Space Sci. Rev.* **180**, 101 (2013).

74. E.V. Savchenko, I.V. Khyzhniy, S.A. Uyutnov, A.N. Ponomaryov, G.B. Gumenchuk, and V.E. Bondybey, *Proc. Phys.* **76**, 111 (2015).

75. V.V. Khmelenko, I.N. Krushinskaya, R.E. Boltnev, I.B. Bykhalo, A.A. Pelmenev, and D.M. Lee, *Fiz. Nizk. Temp.* **38**, 871 (2012) [*Low Temp. Phys.* **38**, 688 (2012)].

76. H.H. Hwang, J.K. Olthoff, R.J. Van Brunt, S.B. Radovanov, and M.J. Kushner, *J. Appl. Phys.* **79**, 93 (1996).

77. J. Marbach, F.X. Bronold, and H. Fehske, *Eur. Phys. J. D* **66**, 106 (2012).

78. R.J. Loveland, P.G. Le Comber, and W.E. Spear, *Phys. Rev. B* **6**, 3121 (1972).

79. L.K. Randenlya, X.K. Zeng, R.S. Smith, and M.A. Smith, *J. Phys. Chem.* **93**, 8031 (1989).

80. A. Lofthus and P.H. Krupenie, *J. Phys. Chem. Ref. Data* **6**, 113 (1977).

81. V.F. Elesin, N.N. Degtyarenko, K.S. Pazhitnykh, and N.V. Matveev, *Russ. Phys. J.* **52**, 1224 (2009).

82. V.A. Apkarian and N. Schwentner. *Chem. Rev.* **99**, 1481 (1999).

83. I.Ya. Fugol', Yu.B. Poltoratski, and Yu.I. Rybalko, *Fiz. Nizk. Temp.* **4**, 1048 (1978) [*Sov. J. Low Temp. Phys.* **4**, 496 (1978)].

84. P.T. McColgan, A. Meraki, R.E. Boltnev, D.M. Lee, and V.V. Khmelenko, *J. Phys. Chem. A* **121**, 9045 (2017).

85. F. Cacace, G. de Petris, and A. Troiani, *Science* **295**, 480 (2002).

86. F. Cacace, *Chemistry A Eur. J.* **8**, 3839 (2002).

87. E. E. Rennie and P.M. Mayer, *J. Chem. Phys.* **120**, 10561 (2004).

88. M.H. Moore and R.L. Hudson, *Icarus* **161**, 486 (2003).

89. N. Weinberger, J. Postler, P. Scheier, and O. Echt, *J. Phys. Chem. C* **121**, 10632 (2017).

90. A.A. Friedmann, S. Nizkorodov, E.J. Bieske, and J.P. Maier, *Chem. Phys. Lett.* **224**, 16 (1994).

91. L.S. Farenzena, P. Iza, R. Martinez, F.A. Fernandez-Lima, E. Seperuelo Duarte, G.S. Faraudo, C.R. Ponciano, E.F. da Silveira, M.G.P. Homem, A. Naves de Brito, and K. Wien, *Earth, Moon, and Planets* **97**, 311 (2005).

92. V. Zhaunerchyk, W.D. Geppert, E. Vigren, M. Hamberg, M. Danielsson, M. Larsson, R.D. Thomas, M. Kaminska, and F. Österdahl, *J. Chem. Phys.* **127**, 014305 (2007).

93. J.L. Fox and A. Dalgarno, *J. Geophys. Res.* **88**, 9027 (1983).

94. *Formation and Trapping of Free Radicals*, A.M. Bass and H.P. Broida (eds.), Academic Press, New York (1960).

95. V.A. Slusarev, Yu.A. Freiman, I.N. Krupskii, and I.A. Burakhovich, *Phys. Status Solidi B* **54**, 745 (1972).

96. D.S. Tinti and G.W. Robinson, *J. Chem. Phys.* **49**, 3229 (1968).

97. N. van Veen, P. Brewer, P. Das, and R. Bersohn, *J. Chem. Phys.* **77**, 4326 (1982).

98. K. Carleton, K. Welge, and S. Leone, *Chem. Phys. Lett.* **115**, 492 (1985).

99. Y.S. Cao and R. Johnsen, *J. Chem. Phys.* **95**, 7356 (1991).

100. S F. Adams, C.A. DeJoseph, Jr., and J.M. Williamson, *J. Chem. Phys.* **130**, 144316 (2009).

101. M. Sauer and W. Mulac, *J. Chem. Phys.* **55**, 1982 (1971).

102. A.H. Hamdani, Z. Shen, Y. Dong, H. Gao, and Z. Ma, *Chem. Phys. Lett.* **325**, 610 (2000).

103. Yu.S. Doronin, M.Yu. Libin, V.N. Samovarov, and V.L. Vakula, *Phys. Rev. A* **84**, 023201 (2011).

Нові тенденції в спектроскопії твердого азоту
(Огляд)

О. Савченко, І. Хижний, V. Bondybey

Цей огляд представляє нові тенденції в емісійній спектроскопії твердого азоту. Обговорюється розвинений підхід до вивчення зарядових центрів та їх ролі в радіаційно-індукованих явищах і релаксаційних процесах. Розроблена емісійна спектроскопія включає в себе корельоване в реальному часі детектування декількох релаксаційних емісій — оптичних фотонів, електронів та емісію частинок. Наведено основні деталі цього підходу, що застосовується при дослідженні попередньо опромінених електронним пучком твердого азоту й азот-гелієвих нанокластерів, вирощених методом газоструйної конденсації. Коротко подані нові методи — нестаціонарна люмінесценція і нестаціонарна десорбція, призначені для вивчення реакцій іон-електронної рекомбінації. Узагальнено недавні результати, отримані з використанням цього підходу і методів емісійної спектроскопії, для вивчення пов'язаних з зарядом явищ у конденсованому азоті. Основну увагу приділено виявленню багатоатомних іонних центрів, що містять чотири і три атоми азоту: N_4^+, N_3^+, N_3^-. Обговорюється їх роль в радіаційних явищах і релаксаційних процесах, зокрема десорбції.

Ключові слова: твердий азот, аніони і катіони азоту, реакції рекомбінації, нейтралізація, тетраазот, десорбція.

Новые тенденции в спектроскопии твердого азота
(Обзор)

Е. Савченко, И. Хижный, V. Bondybey

Этот обзор представляет новые тенденции в эмиссионной спектроскопии твердого азота. Обсуждается развитый подход к изучению зарядовых центров и их роли в радиационно-индуцированных явлениях и релаксационных процессах. Разработанная эмиссионная спектроскопия включает в себя коррелированное в реальном времени детектирование нескольких релаксационных эмиссий — оптических фотонов, электронов и эмиссию частиц. Приведены основные детали этого подхода, применяемого при исследовании предварительно облученных электронным пучком твердого азота и азот-гелиевых нанокластеров, выращенных методом газоструйной конденсации. Кратко представлены новые методы — нестационарная люминесценция и нестационарная десорбция, предназначенные для изучения реакций ион-электронной рекомбинации. Обобщены недавние результаты, полученные с использованием этого подхода и методов эмиссионной спектроскопии, для изучения связанных с зарядом явлений в конденсированном азоте. Основное внимание уделено обнаружению многоатомных ионных центров, содержащих четыре и три атома азота: N_4^+, N_3^+, N_3^-. Обсуждается их роль в радиационных явлениях и релаксационных процессах, в частности десорбции.

Ключевые слова: твердый азот, азотные анионы и катионы, реакции рекомбинации, нейтрализация, тетраазот, десорбция.